

1 **Fractions of Different Young Water Ages are Sensitive to Discharge and Land Use – an**
2 **Integrated Analysis of Water Age Metrics under Varying Hydrological Conditions for**
3 **Contrasting Sub-Catchments in Central Germany**

4 **Christina F. Radtke¹, Stefanie R. Lutz², Christin Mueller¹, Ralf Merz¹, Rohini Kumar³,**
5 **Kay Knoeller¹**

6 ¹ Helmholtz-Centre for Environmental Research UFZ, Department of Catchment Hydrology,
7 Germany

8 ² Copernicus Institute of Sustainable Development, Utrecht University, the Netherlands

9 ³ Helmholtz-Centre for Environmental Research UFZ, Department of Computational
10 Hydrosystems, Germany

11 Corresponding author: Christina F. Radtke (christina.radtke@ufz.de)

12

13 **Key Points:**

- 14 • High-frequency water isotopic signatures can unravel water age changes during short-
15 term hydrologically varying conditions
- 16 • Young water in stream flow is sensitive to discharge variations under changing climatic
17 conditions
- 18 • Landscape structures affect the young water contributions to stream flow with higher
19 Fyw for agricultural catchments

20 **Abstract**

21 With ongoing climate change and more frequent high flows and droughts, it becomes inevitable
22 to understand potentially altered catchment processes under changing climatic conditions. Water
23 age metrics such as median transit times and young water fractions are useful variables to
24 understand the process dynamics of catchments and the release of solutes to the streams. This
25 study, based on extensive high-frequency stable isotope data, unravels the changing contribution
26 of different water ages to stream water in six heterogeneous catchments, located in the Harz
27 mountains and the adjacent northern lowlands in Central Germany. Fractions of water up to 7
28 days old (Fyw7), comparable with water from recent precipitation events, and fractions of water
29 up to 60 days old (Fyw60) were simulated by the tran-SAS model. As Fyw7 and Fyw60 were
30 sensitive to discharge, an integrated analysis of high and low flows was conducted. This revealed
31 an increasing contribution of young water for increasing discharge, with larger contributions of
32 young water during wet spells compared to dry spells. Considering the seasons, young water
33 fractions increased in summer and autumn, which indicates higher contributions of young water
34 after prolonged dry conditions. Moreover, the relationship between catchment characteristics and
35 the water age metrics revealed an increasing amount of young water with increasing agricultural
36 area, while the amount of young water decreased with increasing grassland proportion. By
37 combining transit time modelling with high-frequency isotopic signatures in contrasting sub-
38 catchments in Central Germany, our study extends the understanding of hydrological processes
39 under high and low flow conditions.

40 **1 Introduction**

41 With an expected increase in the frequency of heavy rainfall as well as longer dry periods due to
42 climate change (Kundzewicz et al., 2014), it becomes more and more important to understand
43 the hydrological processes during wet and dry spells as well as the age composition of water
44 (Wilusz et al., 2017). Thanks to the use of tracer data such as isotopic signatures of water to
45 unravel the water age (e.g. median transit time and fraction of young water), our understanding
46 of hydrological processes and the contribution of different water sources and their respective
47 water ages has been improved. Water age metrics such as median transit times and fractions of
48 young water are widely used tools to understand the hydrological pathways of catchments of

49 different sizes. Knowledge of hydrological pathways is an inevitable prerequisite to understand
50 and predict water and pollutant fluxes and pollutant legacies. The composition of different water
51 ages can be simulated by models (e.g. Hrachowitz et al., 2009; Soulsby et al., 2015; Benettin and
52 Bertuzzo, 2018; Kuppel et al., 2018) or purely derived from tracer data (e.g. Kirchner, 2016a;
53 Kirchner, 2016b; Jasechko et al., 2016; Lutz et al., 2018).

54 In studies where the water age is estimated, low-frequency tracer data in timesteps of weekly or
55 monthly data can be used to get an impression about general hydrological processes in
56 catchments (e.g. Lutz et al., 2018; Borriero et al., 2022). However, as shown by von Freyberg et
57 al. (2017) and von Freyberg et al. (2018), sampling frequencies of daily and sub-daily resolutions
58 can provide more detailed information about short-term hydrological processes such as storm
59 runoff events. Lutz et al. (2018) investigated several catchments in the Bode watershed, in
60 central Germany with the focus on estimating fractions of young water with monthly isotopic
61 signatures of water to improve transit time distribution estimates. They found that mean ages of
62 river water range between 9.6 months and 5.6 years depending on catchment characteristics.
63 However, one limitation of the application of low-frequency (i.e. weekly or monthly) tracer data
64 is the insufficient representation of the short-term dynamics such as high flow events and their
65 corresponding hydrological processes (Stockinger et al., 2016, von Freyberg et al., 2018). In
66 contrast, von Freyberg et al. (2017) and von Freyberg et al. (2018) estimated fractions of young
67 water in several Swiss catchments in a daily to sub-daily resolution of tracer data to investigate
68 relationships between young water fractions and catchment characteristics as well as climatic
69 conditions such as storm runoff. Few studies have analyzed the water age in catchments with
70 high resolution isotope data sets during hydrologically divergent periods (e.g., von Freyberg et
71 al., 2017, von Freyberg et al., 2018). Knapp et al. (2019) showed in their analysis of new water
72 fractions and transit time distributions at the Plynlimon experimental catchments in mid-Wales
73 that estimates of water age metrics are affected by sampling frequency. Stream flow isotopic
74 signatures are more damped with lower sampling frequency, which causes a strong difference
75 between water age estimates derived from 7-hour and weekly tracer data (Knapp et al., 2019).
76 Especially, for the analysis of water from previous precipitation events, von Freyberg et al.
77 (2017) showed the relevance of high-resolution isotopic signatures for water age estimates. In a
78 sampling interval of 30 minutes, stream water isotopic signatures were analyzed to estimate
79 event water for eight storm events, which demonstrated the high variability during different

80 storm events as well as a more precise estimation of event water with high-frequency isotope
81 data compared with aggregated isotope data for lower sampling resolutions (von Freyberg et al.,
82 2017). This highlights the potential of high-frequency tracer data applications to understand
83 hydrological processes and their variability during varying climatic conditions such as high and
84 low flows and furthermore implies that that more research is needed in this regard.

85 In view of ongoing and predicted climate change impacts resulting in more frequent high
86 intensity precipitation events and associated storm runoff as well as longer dry periods, there is
87 an urgent need to gain more information about the underlying processes and sources of water
88 during hydrologically divergent periods. To unravel hydrological processes and their
89 dependencies, studies focused on the relation between water age and catchment characteristics
90 such as catchment area, soil type, elevation, land use as well as hydrological indices such as
91 rainfall intensity and discharge (Soulsby et al., 2006; Hrachowitz et al., 2009; Tetzlaff et al.,
92 2009; Jasechko et al., 2016; Wilusz et al., 2017; Lutz et al., 2018; von Freyberg et al., 2018a,
93 Dimitrova-Petrova et al., 2020, Jutebring Sterte et al., 2021). Jasechko et al. (2016) analyzed
94 young water fractions of 254 watersheds globally with regard to catchment characteristics. The
95 analysis revealed high contributions of young water (30%) for most of the catchments with
96 higher young water fractions for agriculturally dominated catchments. On the one hand, these
97 studies highlight the dependency of flow paths and water sources on catchment characteristics.
98 On the other hand, they emphasize the need to understand this interconnectivity in more detail.
99 Most recent studies have investigated the overall relationship between the water age and
100 catchment characteristics, but so far there are very few studies only focusing on the role of water
101 age during varying discharge related to high and low flows (von Freyberg et al., 2017, von
102 Freyberg et al., 2018b). To overcome the blind spot on short term hydrological dynamics of
103 previous studies linking water age distribution based on low-frequency data to climate and
104 landscape features, this study uses high-frequency isotope data and transit time modelling to
105 reveal the difference of age compositions during varying flow conditions in streams,
106 investigating six contrasting sub-catchments within the Bode watershed in Central Germany. We
107 are particularly interested in understanding how stream water age is changing between
108 hydrologically divergent periods such as wet and dry spells and how this is controlled by
109 catchment characteristics. On the basis of an exceptionally extensive high-frequency water stable
110 isotope data set provided by an elaborate isotope monitoring program, the aim of our

111 investigation is (i) to understand how the age distribution of stream water is influenced during
112 hydrologically divergent periods such as wet and dry spells, and (ii) to characterize the effect of
113 catchment characteristics on stream water age during wet and dry spells. These analyses will
114 allow us to inspect the relationship between water age distributions and landscape structures to
115 support a better understanding of flow paths under varying hydrological conditions that occur
116 with the projected climate change. Such understanding is of extreme relevance for the prediction
117 of potential nutrient losses and of changed fluxes and legacies of pollutants that may harm the
118 ecosystems.

119 **2 Materials and Methods**

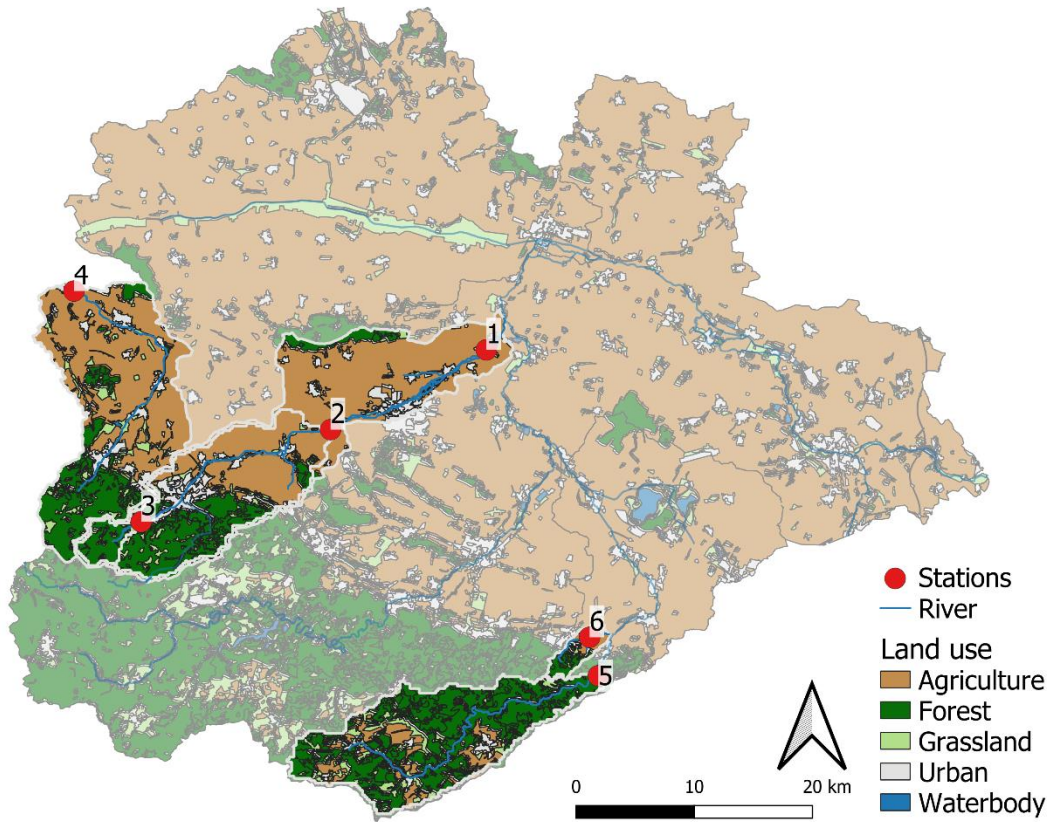
120 **2.1 Study area and data**

121 The intensively studied Bode catchment is located in the Harz mountains and the adjacent
122 northern lowlands in Central Germany (Wollschläger, Attinger et al. 2016, Lutz, Krieg et al.
123 2018). The mesoscale, lower-mountain range Bode catchment is part of the Elbe river basin and
124 ranges between 55 and 1100 m above sea level showing a strong gradient in landscape
125 characteristics from forested headwater catchments to intensively cultivated lowland catchments.
126 It has a humid climate with a mean annual temperature about 9 °C and mean annual rainfall of
127 660 mm, ranging spatially between 450 and 1600 mm. There are several sub-catchments such as
128 the Selke basin or the Holtemme basin where many studies with respect to water fluxes and
129 water quality have been conducted (e.g., Wollschläger, Attinger et al. 2016; Lutz, Krieg et al.
130 2018; Borriero et al., 2022). In this study, we focus on six sub-catchments within the Bode
131 watershed that differ in their size and catchment characteristics such as land use, geology or
132 elevation (Figure 1 and Table 1). An elaborate monitoring program was conducted to provide
133 extensive high-frequency isotope data sets. Automatic samplers specifically designed and proven
134 to collect water samples for isotope analyses avoiding any evaporation effects (Michelsen et al.,
135 2019) were set up at the outlets of five catchments. Aside from the stream water autosamplers,
136 five autosamplers were set up to collect high-frequency precipitation samples. Furthermore,
137 stream water samples at one location (Ilse) and precipitation samples at two locations (Ilse,

138 Meisdorfer Sauerbach) were collected manually on a daily base by citizen scientists who were
139 appointed for the monitoring program.

140 Topographic indices such as elevation, slope and topographic wetness index (TWI) were
141 calculated using the Saga toolbox in QGIS version 3.18.1. Land use shares are taken from Corine
142 Landcover 5 ha (GeoBasis-DE / BKG, 2018). Hydroclimatic indices such as annual average
143 discharge were obtained from discharge measuring stations provided by the Landesbetrieb für
144 Hochwasserschutz und Wasserwirtschaft (Landesbetrieb für Hochwasserschutz und
145 Wasserwirtschaft, 2022). Annual average precipitation is obtained from measuring stations
146 operated by the Deutsche Wetterdienst (DWD, 2021), whereas baseflow index (BFI) is
147 calculated using the daily discharge datasets of all six catchments and the hydroEvents package
148 (<https://CRAN.R-project.org/package=hydroEvents>) in R using version 4.0.5.

149



150

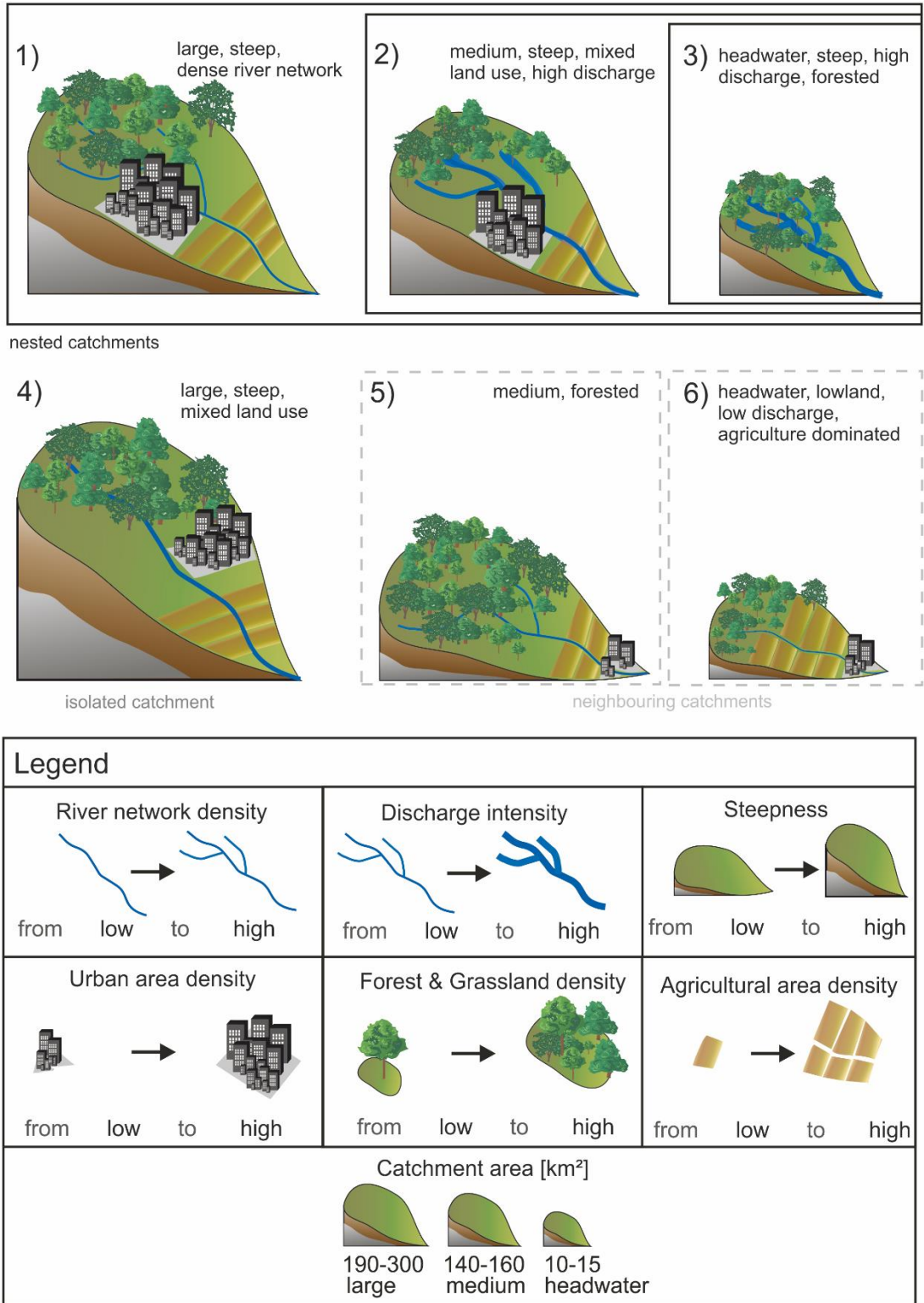
151 Figure 1: Selected catchments from the Harz mountains and the adjacent northern lowlands with
152 their respective land use, where the Stations indicate the locations of both, the stream water and
153 precipitation sampling

154 Table 1: Catchment characteristics with TWI as topographic wetness index and BFI as baseflow index considering time series between
 155 2010 and 2021

Catchment characteristics	1 (Nienhagen)	2 (Mahndorf)	3 (Steinerne Renne)	4 (Ilse)	5 (Selke)	6 (Meisdorfer Sauerbach)
Area [km ²]	282	142.86	13.37	194	157	11.5
Elevation [m a.s.l.]	84-863	134-863	300-863	97-1138	193-576	170-353
Forest [%]	23	25	33	22	31	36
Grassland [%]	33	37	67	40	44	15
Agriculture [%]	18	13	0	19	13	27
Urban [%]	25	24	0	19	11	22
Soil type	Chernozem, brown earth, gley soils, podzols, luvisols	Brown earth, luvisols, chernozem sub-types, podzols	Brown earth podzol with mixtures of clay	Luvisols, gley soils, podzol-brown earth, chernozem, brown earth	Brown earth, luvisols	Brown earth, luvisols, gley soils
TWI (mean)	11-28 (16)	11-27 (15)	11-20 (15)	11-24 (16)	12-23 (15)	12-23 (15)
Slope [°] (mean)	0.01-21.29 (2.9)	0.01-21.29 (4.04)	0.39-20.87 (7.95)	0.01-25.82 (2.98)	0.16-17.55 (3.77)	0.03-6.55 (2.31)
Flow path length [km]	42.66	23.09	2.07	28.68	30.12	7.37
Annual avg. discharge [mm]	102	208	529	160	128	40
BFI	0.48	0.62	0.55	0.60	0.55	0.26
Annual avg. precipitation [mm]	424	465	576	538	547	548

157 The sub-catchments selected for high-frequency isotopic sampling cover a wide range of climate
158 and landscape characteristics of the Bode river basin. The largest sub-catchment is a hilly
159 anthropogenically impacted catchment (Nienhagen catchment, 282 km²) (Fig. 2, catchment 1),
160 showing the highest density of river network and including lowlands with intensive agriculture
161 (18%) and urban area (25%). The Mahndorf catchment (142.86 km²) (Fig. 2, catchment 2) is
162 nested within the Nienhagen catchment and shows some anthropogenic impacts, such as urban
163 area (24%) and agricultural crop land (13%). One of the smallest sub-catchments is Steinerne
164 Renne (13.37 km²) (Fig. 2, catchment 3), a typical German mid-elevation mountain range
165 headwater catchment with dominant forest (33%) and grassland (67%) cover. The catchment
166 may be seen as a pristine head water catchment, as no agricultural fields and no urban areas are
167 located within the catchment. With 529 mm the discharge is highest in the Steinerne Renne
168 catchment compared to the other catchments. The Steinere Renne is part of the Mahndorf
169 catchment. The mountainous agriculturally dominated Ilse catchment (194 km²) (Fig. 2,
170 catchment 4) has the highest elevation range (ranging between 97 and 1138 m) forest (22%) and
171 grassland (40%) dominating the upper part of the catchment and a high density of agricultural
172 area (19%) in the lowlands. Compared to the Steinerne Renne and Mahndorf catchment, the Ilse
173 catchment shows less discharge (160 mm). With more forested (31%) and grassland (44%) area,
174 the Selke catchment (157 km²) (Fig. 2, catchment 5) shows less anthropogenic impacts than the
175 Mahndorf catchment. The Selke catchment is located in the lower part of the Harz mountains,
176 but is still hilly and mainly forested. A neighboring catchment to the Selke is the Meisdorfer
177 Sauerbach catchment (Fig. 2, catchment 6). It is an agriculturally dominated headwater
178 catchment in the lowlands of the Harz mountains. This catchment is the smallest (11.5 km²) from
179 all investigated catchments and has the lowest annual average discharge (40 mm).

180



181

182 *Figure 2: Illustration of all six catchments investigated, considering their most meaningful*

183 *catchment characteristics*

184 2.2 Sampling

185 Water samples of stream water (grab samples) and precipitation (composite samples) were
186 collected in a monthly frequency from 2013 to 2017 for the catchments 5 and 6, and from 2013
187 to 2019 for the catchments 1-3. In 2020 autosamplers were set up in the catchments 1-3 and 5 to
188 collect daily water samples of precipitation and stream water. In catchment 6 stream water was
189 collected with an autosampler since 2020 and precipitation was collected manually. At the
190 sampling location of catchment 4, manual samples have been taken daily from both precipitation
191 and stream water since 2020. Event water samples were taken with the autosampler at sub-daily
192 timesteps (4 hours to 8 hours) whenever heavy rainfall was predicted to occur following a public
193 weather forecast. Stream water samples were taken via a pump as grab samples at specific time
194 steps: daily samples were taken at 3 pm, and sub-daily samples were taken every 4, 6 or 8 hours,
195 depending on the chosen program. Precipitation was sampled using a collector that switches the
196 position of the sampling bottle at each programmed time step: 4-8 hours during a predicted
197 precipitation event and 24 hours during daily sampling.

198 2.3 Laboratory analysis

199 Water samples were filtered through a 0.45 μm filter. A liquid isotope analyzer (Picarro L2120-
200 I) was used for duplicate measurements of stable isotopic signatures of water. By using replicate
201 (20x) analysis of internal standards calibrated to VSMOW and Standard Light Antarctic
202 Precipitation (SLAP) certified reference materials, the samples were normalized to the VSMOW
203 scale. The analytical uncertainty of $\delta^{18}\text{O}$ and $\delta^2\text{H}$ were $\pm 0.1 \text{ ‰}$ and $\pm 0.6 \text{ ‰}$ respectively. The
204 isotopic ratios are expressed in delta notation relative to Vienna Standard Mean Ocean Water
205 (VSMOW) for the oxygen and hydrogen isotope signatures of water:

$$\delta_{\text{sample}}[\text{‰}] = \left(\frac{R_{\text{sample}}}{R_{\text{standard}}} - 1 \right) \times 1000 \quad (1)$$

206 Due to higher measurement precision, the isotopic signature of $\delta^{18}\text{O}$ of water is used for the
207 following investigations.

208 2.4 Data preparation

209 The model used in this study to estimate transit times of water requires continuous hydrological
 210 and tracer input data. For this purpose, we used hydrological outputs from a well-established
 211 Mesoscale Hydrological Model (mHM) (Samaniego et al., 2010; Kumar et al., 2013). The model
 212 was established at a 1 km spatial resolution to simulate continuous datasets of daily discharge
 213 and evapotranspiration. mHM has been thoroughly evaluated in past studies (see e.g., Zink et al.,
 214 2017; Mueller et al., 2016). Meteorological forcings such as precipitation and air temperature to
 215 drive the model were acquired from German Weather Service, DWD (DWD, 2021).

216 To consider the change of isotopic signatures in precipitation with elevation for all catchments
 217 investigated in this study, ordinary kriging of isotopic signatures of precipitation with elevation
 218 as external drift was conducted in R version 4.0.5. All precipitation isotope sampling locations
 219 that are located in the investigated catchments were used for kriging. The isotopic signature per
 220 day was extracted for each catchment as spatial mean of the kriged values over the catchment
 221 area for the following transit time modelling.

222 2.5 Transit time modelling

223 To model water transit times and water ages, the numerical model tran-SAS v1.0 (Benettin and
 224 Bertuzzo 2018) was set up for each catchment. By using tracer data such as isotopic signatures of
 225 water in combination with hydrological data (precipitation, evaporation and discharge), the tran-
 226 SAS model is able to simulate age metrics such as the daily median transit time as well as
 227 fractions of young water by applying storage age selection functions (SAS).

228 The conceptualization of each catchment is based on a single storage $S(t)$ with a water-age
 229 balance that can be expressed as follows (Benettin and Bertuzzo, 2018):

230

$$S(t) = S_0 + V(t) \quad (2)$$

$$\frac{\partial S_T(T, t)}{\partial t} + \frac{\partial S_T(T, t)}{\partial T} = P(t) - Q(t) * \Omega_Q(S_T, t) - ET(t) * \Omega_{ET}(S_T, t) \quad (3)$$

$$\text{Initial condition: } S_T(T, t = 0) = S_{T_0} \quad (4)$$

$$\text{Boundary condition: } S_T(0, t) = 0 \quad (5)$$

231 Where S_0 is the initial storage, $V(t)$ (mm) are the storage variations, $P(t)$ is precipitation
 232 (mm/d), $Q(t)$ is discharge (mm/d) and $ET(t)$ is evapotranspiration (mm/d). $S_T(T, t)$ (mm) is the
 233 age-ranked storage with S_{T_0} (mm) as initial age-ranked storage. The cumulative SAS functions
 234 are described as $\Omega_Q(S_T, t)$ for discharge and $\Omega_{ET}(S_T, t)$ for evapotranspiration.

235 The SAS functions can be expressed as probability density functions with regard to the
 236 normalized age-ranked storage:

237

$$\omega(P_S(T, t), t) = k * (P_S(T, t))^{k-1} \quad (6)$$

$$\omega(P_S(T, t), t) = \frac{(P_S(T, t))^{\alpha-1} * (1 - P_S(T, t))^{\beta-1}}{B(\alpha, \beta)} \quad (7)$$

238 Where the catchment's water age preference for outflow is described by the parameters k , α and
 239 β , while $B(\alpha, \beta)$ is the two-parameter beta function. The catchment has a preference to release
 240 young water if $k < 1$, $\alpha < 1$ and $\beta < 1$. In case of $k > 1$, $\alpha > 1$ and $\beta > 1$, the catchment tends to discharge
 241 old water. No selection preference (i.e., complete water mixing) is described with $k=1$, $\alpha=1$ and
 242 $\beta=1$. For stream water, the beta distribution SAS function (Equ. 7) was applied. Since we do not
 243 focus on the water age for evaporation and due to the lack of tracer data from evapotranspiration,
 244 we applied the time invariant power law function (Equ. 6) to evaporation fluxes for the
 245 completeness of the model. By this, we got four parameters to be evaluated using the fit of
 246 modelled vs. observed streamflow isotope data, i.e., α and β for stream water, β for
 247 evapotranspiration and the initial storage parameter S_0 (Supplement Table 1). A GLUE approach
 248 was conducted to evaluate the 10% best simulations considering the Kling-Gupta-Efficiency
 249 (Gupta, Kling et al. 2009) between observed isotopic signatures in stream and simulated isotopic
 250 signatures in stream (Equ. 8).

251

$$KGE = 1 - \sqrt{(r - 1)^2 + \left(\frac{\sigma_{sim}}{\sigma_{obs}} - 1\right)^2 + \left(\frac{\mu_{sim}}{\mu_{obs}} - 1\right)^2} \quad (8)$$

252 where $\sigma_{(sim/obs)}$ is the standard deviation in observations/simulations and $\mu_{(sim/obs)}$ the mean of
 253 simulation/observation, and r is the linear correlation between observations and simulations.
 254 $KGE=1$ indicates perfect agreement between simulations and observations. For statistical
 255 analysis of the relationship between age metrics and catchment characteristics, the mean value of
 256 the 10% best simulations was calculated for each catchment individually. In addition, the
 257 absolute bias between measured and modelled data was considered for the evaluation of the
 258 performance of the simulated isotopic signature in stream water.

259 2.6 Hydrologically divergent periods and statistical analysis

260 The discharge sensitivity was presented as a valuable tool to investigate the hydrological
 261 behavior of different catchments with each other. Von Freyberg et al. (2018) showed that Fyw
 262 were sensitive to increasing discharge, while each catchment showed different sensitivities of
 263 Fyw to discharge. Therefore, they introduced Fyw-discharge sensitivity as indicator to describe
 264 catchment specific water age dynamics. Gallart et al. (2020) developed this method further by
 265 using an exponential equation (Equ. 9) describing the relationship between Fyw and discharge:

$$Fyw(Q) = 1 - (1 - F_0) * \exp(-Q * S_d) \quad (9)$$

266 With F_0 as virtual Fyw for discharge (Q) being zero and S_d (unit of Q^{-1}) as a new discharge
 267 sensitivity metric (Gallart et al., 2020). Gallart et al. (2020) showed that an exponential equation
 268 is needed to ensure that Fyw cannot be above one even when discharge rises infinitely, and that
 269 for low discharges the curve approximates a linear line (Gallart et al., 2020). The discharge
 270 sensitivity presented by von Freyberg et al. (2018) was described by a linear equation. The
 271 discharge sensitivity of von Freyberg et al. (2018) equals S_d from the exponential equation of
 272 Gallart et al. (2020) as long as Fyw is lower than 1. In our study, Equ. (9) was used for two
 273 different metrics of young water to investigate the sensitivity of young water release in the
 274 catchments as a function of discharge. For comparison with other studies the fraction of water
 275 with an age up to 60 days (Fyw60), which is similar to the young water fraction with an age

276 between 60 and 90 days according to Kirchner (2016), was obtained from the tran-SAS model as
277 well as the fraction of water with an age up to 7 days (Fyw7) to represent recent precipitation
278 water. We obtained the F_0 and S_d parameters with a non-linear analytic Gauss–Newton
279 algorithm by fitting Equation 9 to Fyw7 and Fyw60 from the tran-SAS simulations, respectively.
280 For this, the discharge was separated into 10% percentiles to cover different discharge
281 intensities, because the daily data showed a scatter that was not be able to be represented by the
282 Equ. 9, which plots as exponential curve.

283 To analyze the differing water age behavior in hydrologically divergent periods, we separated the
284 runoff time series into dry and wet spells. We define dry spells as periods with low flow
285 conditions, and wet spells as periods with high flow conditions. There are two common
286 approaches in separating discharge time series. The first is a simple threshold approach
287 categorizing periods above the threshold as wet spells, and periods below the threshold as dry
288 spells (Lang et al., 1999, Sikorska et al., 2015). This approach has the disadvantage that parts of
289 the same rainfall-runoff event may belong to dry spells (e.g. start of the rising limb, end or the
290 recession), while other parts may be categorized as wet spells. For highly seasonal regimes,
291 where seasonal variance in runoff is higher than the variance between rainfall-runoff events and
292 no events, the threshold approach may only be able to classify according to the seasons. A
293 second approach is a classical baseflow filtering approach, where all periods with direct flow
294 components (i.e. rainfall-runoff events) are classified as wet spells (Merz et al., 2006, Ladson et
295 al., 2013). This approach usually tends to lead to very short events.

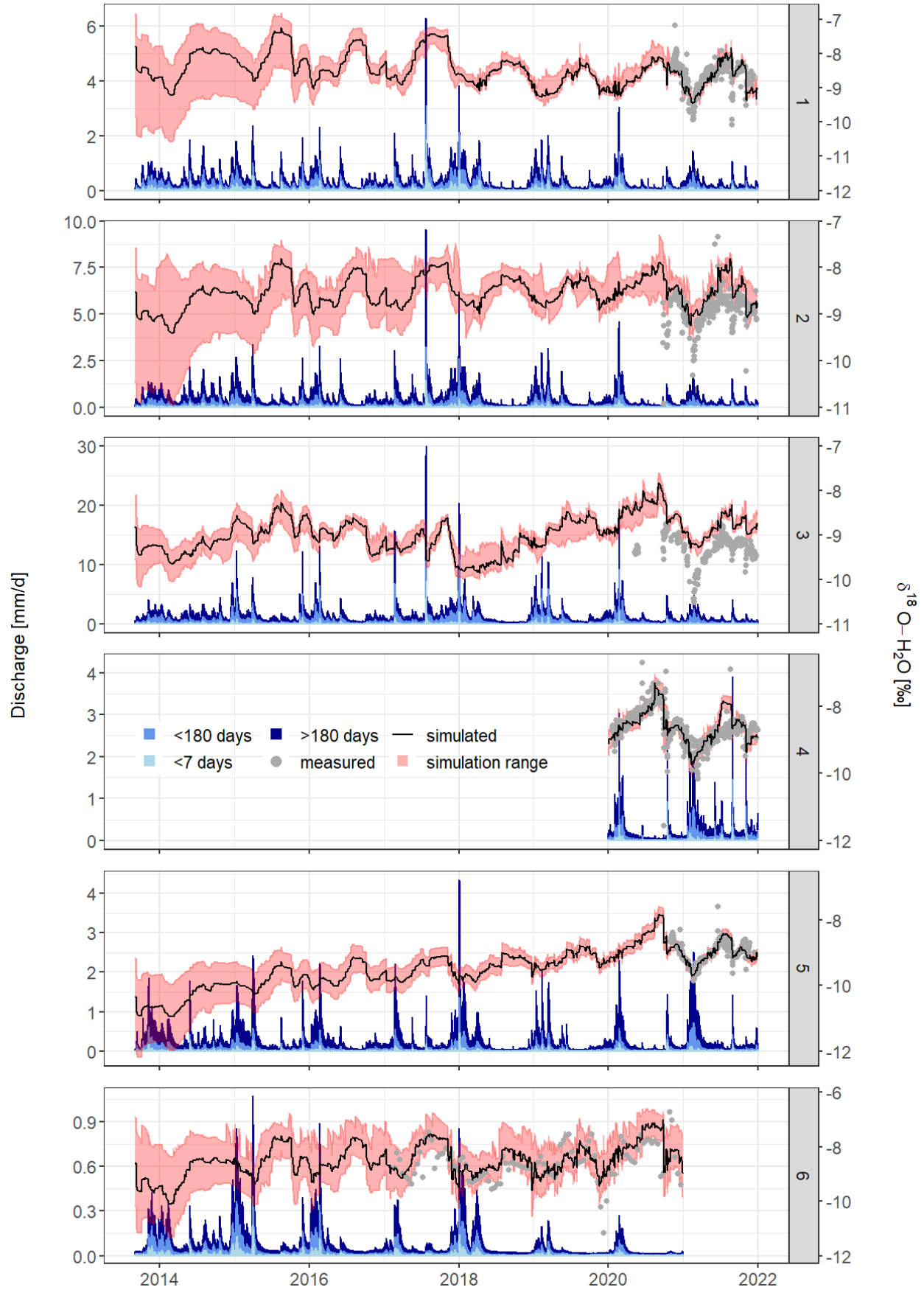
296 In this study we used a combination of both approaches. In a first step, single rainfall-runoff
297 events were identified following the baseflow separation approach of Lyne and Hollick (1979)
298 using R package hydroEvents (Ladson et al., 2013, Kaur et al., 2017, Tang et al., 2017). In a
299 second step, all events with a peak flow in discharge higher than long-term median peak flows
300 were categorized as wet spells, while periods with peak flows under the threshold belong to the
301 category dry spells. By this, each catchment has an individual threshold value for wet spells
302 corresponding to its median peak flow. No event periods were also categorized as dry spells.

303 This approach tends to generate longer contiguous periods of dry and wet spells, while still
304 accounting for single rainfall-runoff events.

305 Wet spells and dry spells were gained from the time series 2013 to 2021, except for the
306 catchment 4, which covers only the years 2020 to 2021, and catchment 6, where the data was
307 available from 2013 to 2020. The relation between water age metrics (median transit time,
308 fractions of different water ages) and catchment characteristics, such as land use share, elevation,
309 slope and some more, of the different catchments were analyzed statistically. To understand how
310 recent precipitation, in particular, affects the stream water age composition, the fraction of water
311 with an age up to 7 days (Fyw7) was investigated in more detail in relation to catchment
312 characteristics.

313 **3 Results and Discussion**

314 3.1 Water age modelling



316 *Figure 3: Discharge with the different fractions of water age in light blue = water age up to 7*
317 *days, medium blue = water age up to 180 days and dark blue = water age more than 180 days*
318 *for the six investigated catchments; the measured isotopic signature of discharge is shown as*
319 *grey dots, while the simulated isotopic signature of discharge gained from the tran-SAS model is*
320 *shown as black line; the range of simulated stream isotopic signature is shown as red shading.*

321 In addition to measured and simulated isotope values, Fig. 3 shows the fraction of three
322 categories of water ages: the fraction of young water up to 7 days (<7 days) highlighting water
323 flow through fast flow paths, water up to 180 days and water older than 180 days, representing
324 water that was stored in the catchments and/or traveled along slow flow paths. The fraction of
325 young water up to 7 days (<7 days) is highest in the agricultural lowland headwater catchment
326 (catchment 6; mean: 0.082 or 8.2 %) and lowest in the pristine forested headwater catchment
327 (catchment 3; mean: 0.032 or 3.2 %), considering the mean of all best simulations and the whole
328 time series. In the forested hilly catchment (catchment 5), the contribution of water older than
329 180 days (>180 days) is highest compared to other catchments (mean: 0.75 or 75 %), which is
330 also reflected by high median transit times (see Figure 7). The hilly anthropogenic and the
331 anthropogenic catchments (catchments 1 and 2, respectively) as well as the agriculturally
332 dominated catchment (catchment 4) have similar proportions of different water ages. The water
333 age contributions of the mountainous agricultural dominated catchment (catchment 4) are in
334 similar ranges as from the hilly anthropogenic (catchment 1) and the anthropogenic (catchment
335 2) catchments.

336 The performance of simulated isotopic signature by tran-SAS is shown in Figure 3, in which the
337 black line shows the mean of all best simulations and the red area reflects the variability of all
338 best simulations. For the catchments 1 (hilly, high anthropogenic impact), 4 (mountainous
339 agriculturally dominated), and 5 (forested, hilly), the simulations generally match the observed
340 values (grey dots in Fig. 3), which is also reflected by high KGE values (KGE = 0.65-0.79) and
341 low absolute biases (absolute bias = -0.09 – 0.09). The 10% best simulations for the catchment 3
342 (pristine forested headwater catchment) show similar KGE values (KGE = 0.63-0.71) but larger
343 biases (absolute bias = -0.58 – 0.49), while for the catchments 2 (high anthropogenic impact) and
344 6 (agricultural lowland headwater catchment) the KGE is lower (KGE = 0.47-0.54), and the bias
345 is visibly higher (absolute bias = -0.74 – 0.48). In catchments 3,5 and 6, the model tends to
346 overestimate isotopic measurements, which has to be considered for interpreting the results.

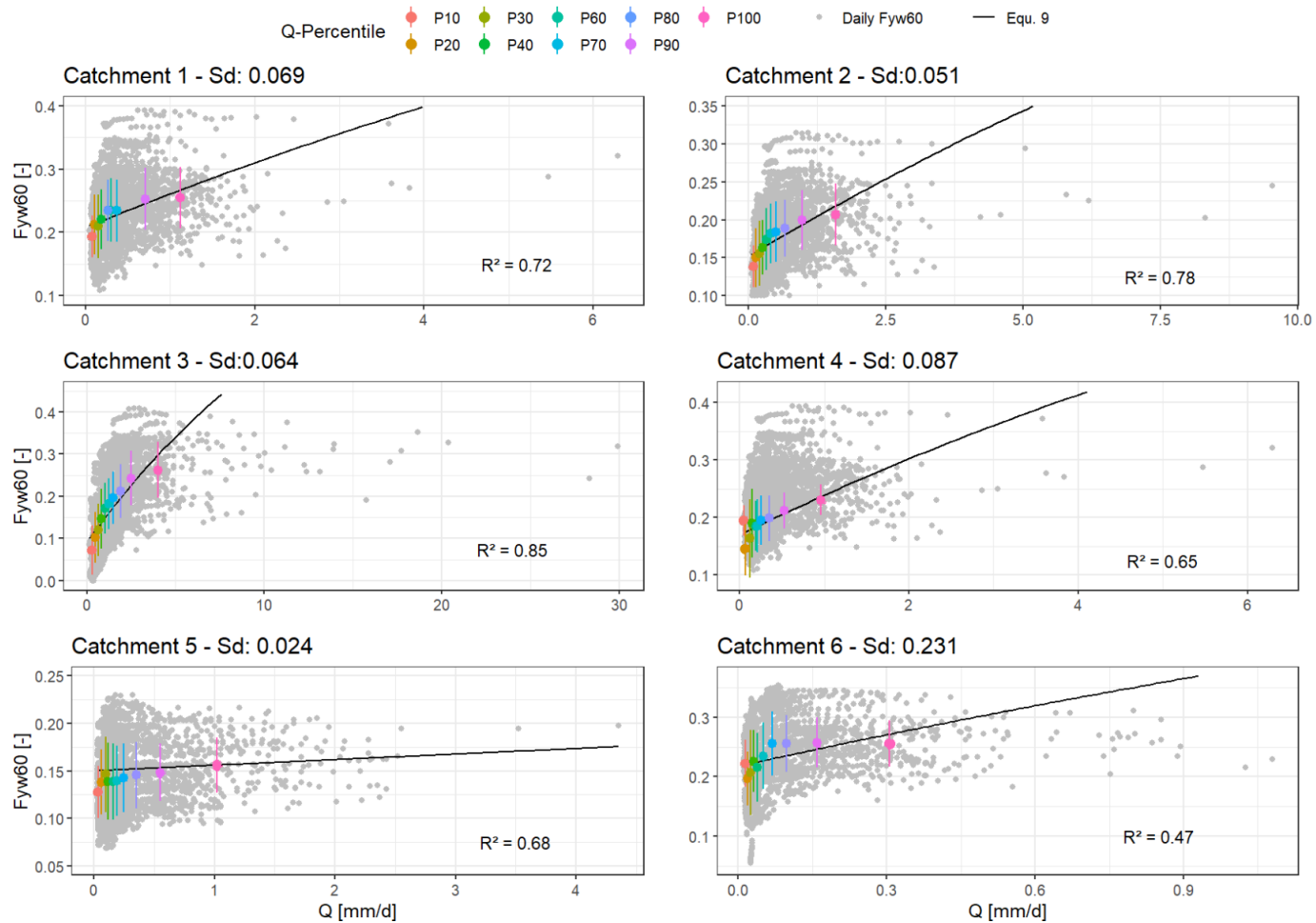
347 3.2 Sensitivity of young water fractions to discharge

348 Figures 4 and 5 display the discharge sensitivity according to Equ. 9 as black line in each plot,
 349 showing positive slope for each catchment. With increasing discharge percentiles, the Fyw60
 350 increases as well, but in different intensities for each catchment. Sd as discharge sensitivity
 351 metric (Gallart et al., 2020) is highest in the agriculturally dominated headwater catchment
 352 (catchment 6; Sd = 0.232) and lowest in the hilly, forested catchment (catchment 5; Sd = 0.024).
 353 The discharge sensitivity of our investigated catchments yielded similar ranges as found in von
 354 Freyberg et al. (2018) and Gallart et al. (2020), except for the agriculturally dominated
 355 headwater catchment (catchment 6) which showed higher discharge sensitivity than all other
 356 catchments (Table 2).

357 *Table 2: Values for F0 and Sd and their standard deviation obtained from Gauss-Newton fitting*
 358 *algorithm using eq. 9 for Fyw7 (water with an age up to 7 days) and Fyw60 (water with an age*
 359 *up to 60 days).*

Catchment	Fyw7		Fyw60	
	F0	Sd	F0	Sd
1	0.043 ± 0.002	0.067 ± 0.005	0.208 ± 0.005	0.069 ± 0.014
2	0.032 ± 0.002	0.036 ± 0.003	0.152 ± 0.006	0.051 ± 0.011
3	0.006 ± 0.001	0.019 ± 0.001	0.092 ± 0.015	0.064 ± 0.010
4	0.034 ± 0.004	0.058 ± 0.011	0.170 ± 0.007	0.087 ± 0.023
5	0.032 ± 0.001	0.028 ± 0.003	0.136 ± 0.002	0.024 ± 0.006
6	0.069 ± 0.004	0.180 ± 0.034	0.218 ± 0.008	0.232 ± 0.087

360

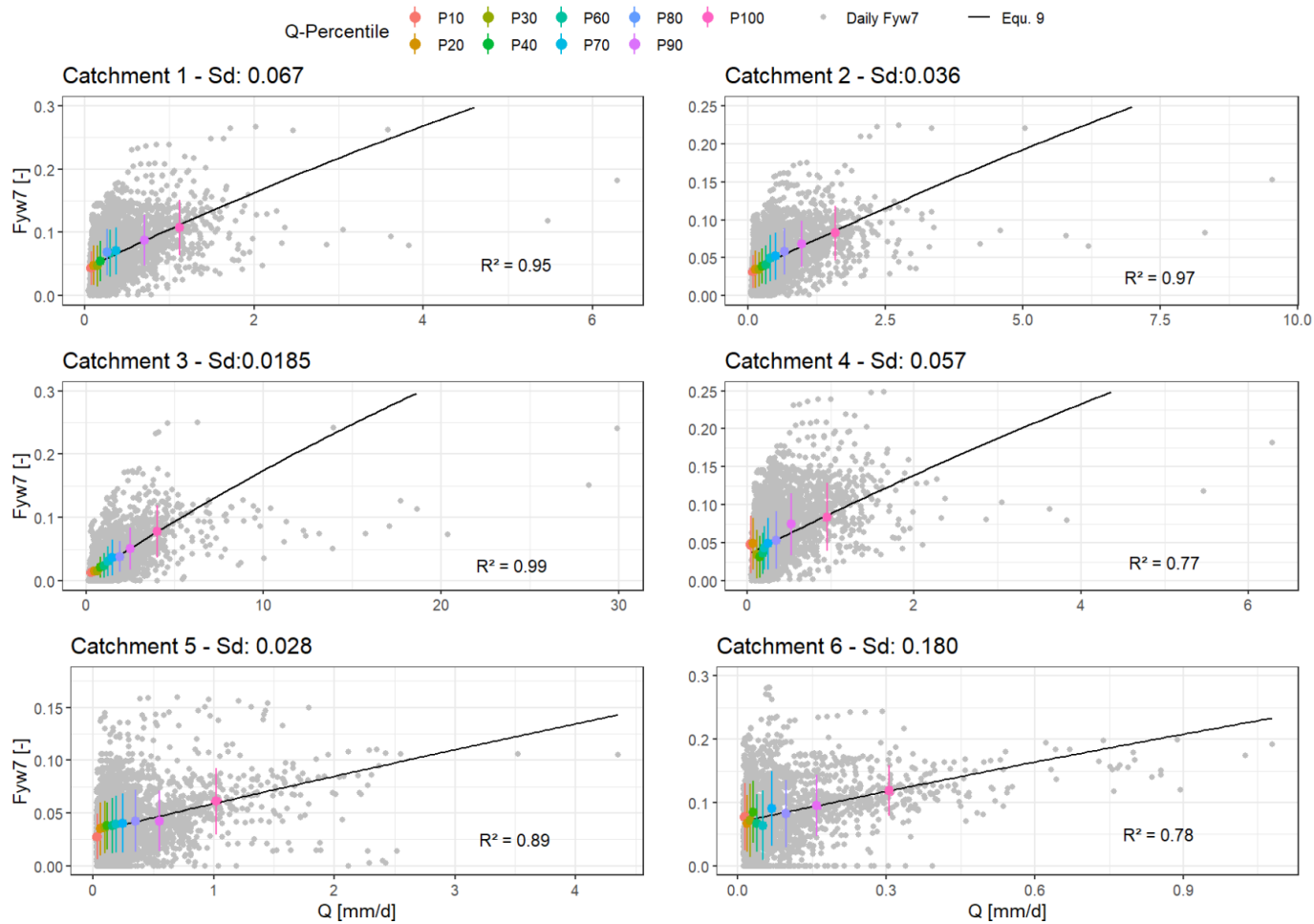


361

362 *Figure 4: Relationship between discharge and the fraction of water with an age up to 60 days (F_{yw60}) with the median discharge (Q*
 363 *[mm/d]) from each percentile and the mean F_{yw60} as well as its standard deviation from each Q -percentile for the whole time series;*
 364 *F_{yw60} of discharge percentiles (P10-P100) are represented as colored points with standard deviation, while the black line represents*
 365 *Equ. 9 to describe the discharge sensitivity (Sd) of the F_{yw60} ; the coefficient of determination (R^2) describes the fit of Equ. 9 on the*
 366 *colored dots.*

367 Considering Fyw7 (Fig. 5), the discharge sensitivity of all catchments is lower compared to the
368 discharge sensitivity of Fyw60 (Fig. 4). For some catchments (i.e., hilly anthropogenic
369 catchment 1 and forested, hilly catchment 5) the difference is small, while for other catchments
370 the difference of the discharge sensitivities is large (pristine forested headwater catchment 3).
371 This means that the Fyw7 is generally less affected by discharge than Fyw60, but it depends on
372 the catchment. Catchments that were characterized by a hilly landscape showed a small
373 difference of the discharge sensitivities of both Fyw7 and Fyw60, while the catchment with the
374 highest discharge showed the largest difference of discharge sensitivities of both Fyw7 and
375 Fyw60. These indications lead us to further investigate catchment's characteristics and their
376 relationship to young water (Fyw7 and Fyw60) in a separate chapter (Chapter 3.5).
377 While Equ. 9 and the discharge sensitivity metric S_d give information about the average
378 behavior of the fractions of different water ages of each catchment, the daily Fyw7 and Fyw60
379 (grey dots) give the opportunity to evaluate their variations with respect to the discharge. Most of
380 the catchments show similar patterns: they have discharge sensitivities of Fyw60 which do not
381 differ strongly across catchments, considering the standard deviation (Catchments 1, 2, 3, 4). The
382 anthropogenic catchment (catchment 2) and the pristine forested headwater catchment
383 (catchment 3) show steeper slopes for Fyw60 than for Fyw7, which indicates that Fyw60 is more
384 sensitive to discharge than Fyw7 in these catchments. Catchments with steep slopes of Fyw60
385 but lower slopes for Fyw7 can be catchments that release water from previous precipitation
386 events (Fyw7) more uniformly, but with increasing discharge the amount of young water up to
387 60 days is released more dominantly. This is in line with findings from von Freyberg et al.
388 (2018b), who investigated the storm runoff response by using event and pre-event water and
389 found out that predominantly pre-event water from shallow water pathways is released during
390 storm runoff with increasing discharge peaks. In our study, the highest discharge sensitivity was
391 found for the agriculturally dominated headwater catchment, which is the smallest catchment
392 investigated. Probably due to the high amount of agricultural land use and associated tile-
393 drainage systems, the catchment is prone to release young water very quickly, which is in line
394 with the daily Fyw60 and Fyw7 values showing the highest fractions compared to all other
395 catchments.
396 The release of young water by catchments that are dominated by agricultural land use was also
397 found by Jasechko et al. (2016), who investigated 254 watersheds globally and found out that the

398 streamflow of most of the catchments consists of 30% young water with predominantly higher
399 amounts of young water for agriculturally dominated catchments. Considering the daily Fyw60
400 and Fyw7, the neighboring catchments (hilly, forested and agriculturally dominated headwater
401 catchments) show a more distributed pattern of the daily Fyw7 and Fyw60 than the other
402 catchments. The high day-to-day variability of different young water fractions indicate that these
403 catchments are more affected by climatic conditions such as dry periods, when water storages
404 that contain more old water can dry out., As a result, more young water is released during high
405 flows after prolonged dry conditions. This assumption is investigated in more detail in the
406 following sections.



407

408 *Figure 5: Relationship between discharge and the fraction of water with an age up to 7 days (Fyw7) with the median discharge (Q*
 409 *[mm/d]) from each percentile and the mean Fyw7 as well as its standard deviation from each Q-percentile from the whole time series;*
 410 *Fyw7 of discharge percentiles (P10-P100) are represented as colored points with standard deviation, while the black line represents*
 411 *Equ. 9 to describe the discharge sensitivity (Sd) of the Fyw7; the coefficient of determination (R²) describes the fit of Equ. 9 on the*
 412 *colored dots.*

413 3.3 The effect of hydrologically divergent periods on discharge age distribution

414 The discharge sensitivity analysis showed that both Fyw7 and Fyw60 are sensitive to discharge
 415 intensities. To better understand how fractions of different water ages are affected during low
 416 flows and high flows und to highlight hydrologically divergent periods, the time series was
 417 separated into dry and wet spells according to their discharge. The results of this separation and
 418 the differences in the number of wet spells between the years and between the single catchment
 419 is shown in table 3.

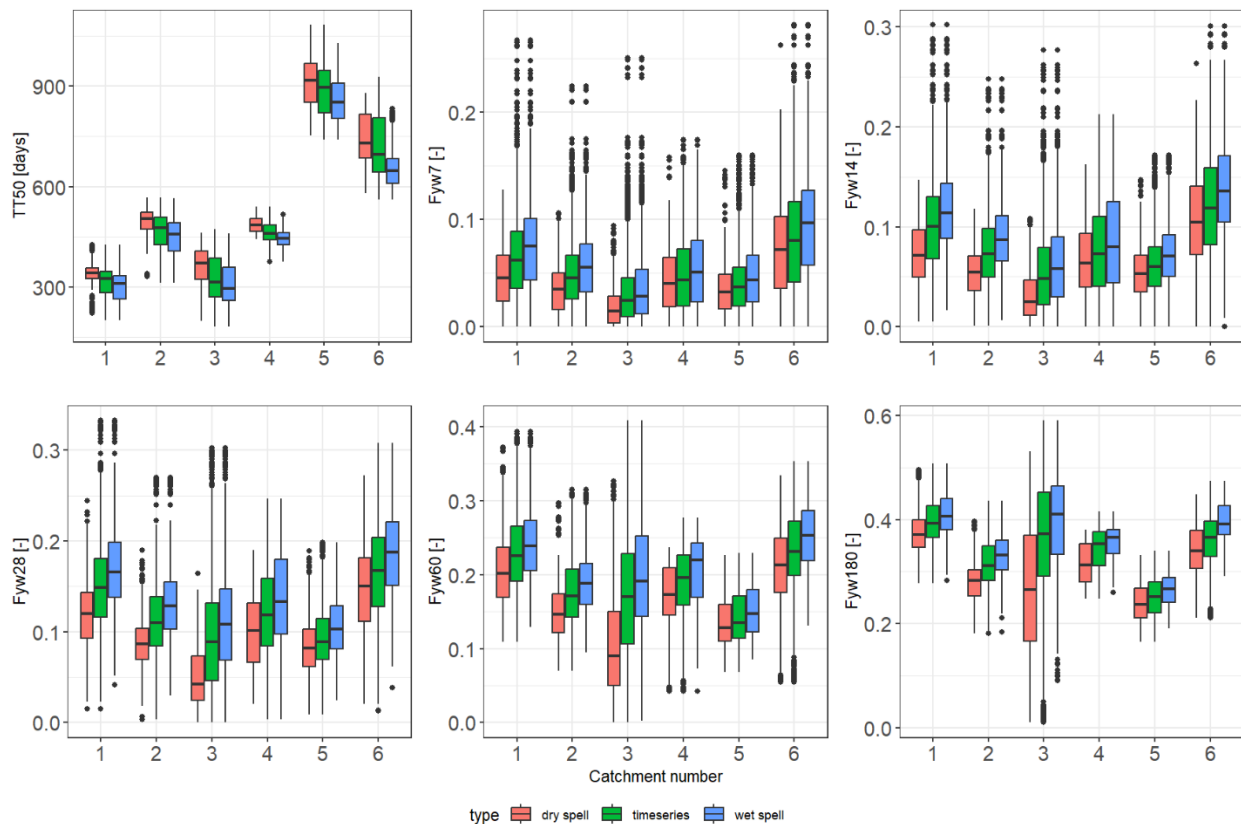
420 *Table 3: The number of wet spells in total and the mean duration of wet spells during the years*
 421 *for the investigated catchments*

Catc hme nt	1		2		3		4		5		6	
	Wet Spell	Mea n durat ion										
Total	43	-	36	-	28	-	10	-	53	-	22	-
Mea n	5	74	4	90	3	97	5	65	6	50	3	83
2013	2	132	1	152	1	117	-	-	4	60	1	136
2014	7	65	7	77	4	103	-	-	11	28	7	74
2015	5	56	4	100	3	77	-	-	5	45	2	115
2016	5	72	4	72	4	97	-	-	7	39	2	96
2017	6	64	6	64	4	95	-	-	6	53	6	49
2018	4	80	3	111	2	144	-	-	4	64	1	80
2019	4	55	3	85	3	96	-	-	5	31	2	46
2020	6	58	5	60	4	71	4	70	3	55	1	65
2021	4	84	3	87	3	71	6	60	6	74	-	-

422 The variation of the mean median transit times (TT50) of all simulations across the study period
 423 varies strongly for the different catchments (Fig. 6). Whereas TT50s are the smallest in the hilly
 424 anthropogenic catchment (catchment 1) and the pristine forested headwater catchment
 425 (catchment 3) with 150 to 450 days, the highest TT50s occur in the neighboring catchments 5
 426 (forested, hilly) and 6 (agricultural lowland headwater) (between 600 and 1000 days). The

427 anthropogenic catchment (catchment 2) and the mountainous agriculturally dominated catchment
 428 (catchment 4) are in the middle of the distribution, covering TT50s of between 300 and 600 days.
 429 In general, the TT50s are smaller during wet spells compared to dry spells. This illustrates the
 430 higher contribution of young water during wet spells compared to dry spells. The Fractions of
 431 young water complement this observation by showing a higher Fyw of up to 7 days during wet
 432 spells for all the catchments, compared to dry spells and the time series in general. This behavior
 433 of more young water holds for all Fyw metrics investigated (i.e., water with an age of up to 14,
 434 28, 60 and 180 days; Fig. 6).

435



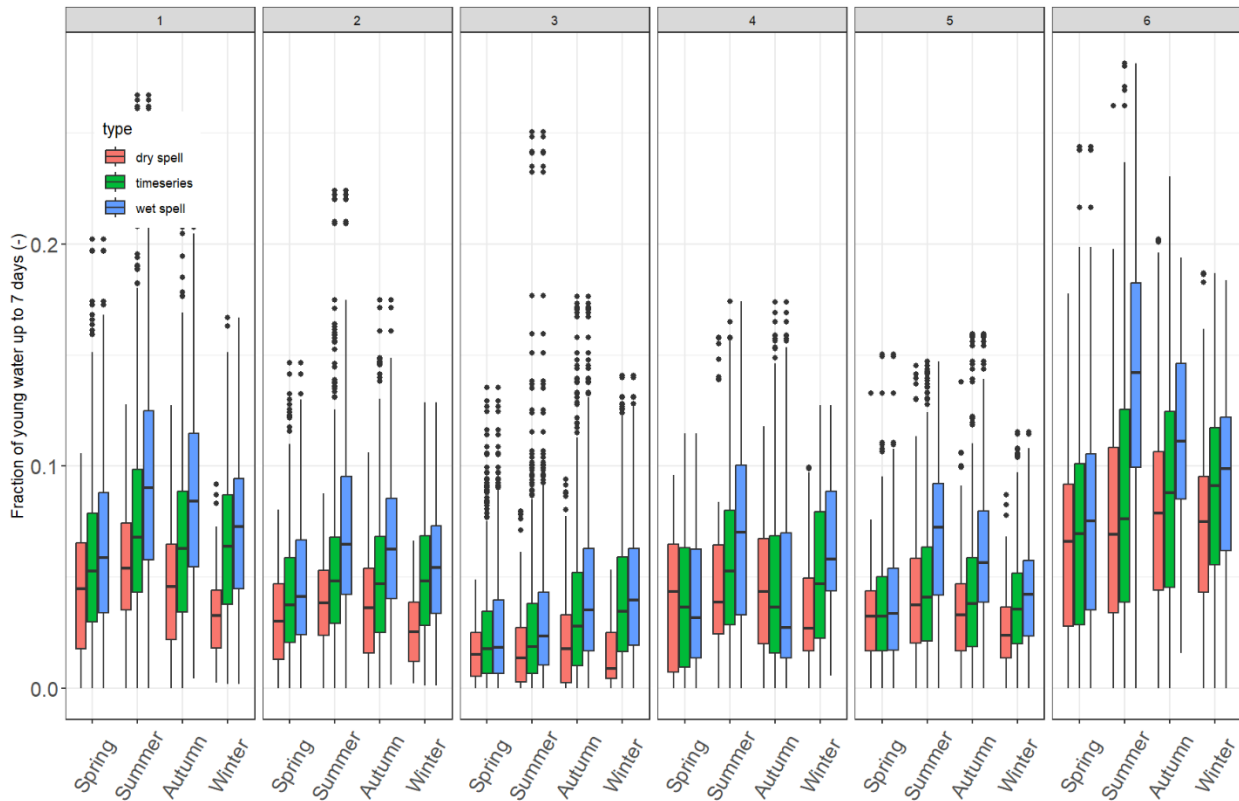
436

437 *Figure 6: The age metrics (TT50 and Fyw7-180) for each catchment during dry spells (red), the*
 438 *whole time series (green) and wet spells (blue).*

439 The higher proportion of young water during wet spells as seen in Figure 6 becomes also
 440 apparent in the different seasons (Figure 7 and 8). All catchments show significantly higher
 441 contributions of young water up to 7 days during wet spells compared to dry spells during all
 442 seasons ($p < 0.05$), except for the mountainous agriculturally dominated catchment (catchment 4)

443 where no significant difference between spring and autumn is obvious. During summer and in
444 some cases during autumn, the relative contribution of Fyw7 to overall discharge is significantly
445 larger than during the other seasons ($p < 0.05$), except for hilly catchments 2, 4 and 6 where no
446 significant difference can be found between summer and winter periods. Also, the pristine
447 forested headwater catchment (catchment 3) does not show a significant difference between
448 summer and spring. Especially the neighboring catchments 5 (forested, hilly) and 6 (agricultural
449 lowland headwater) show increasing Fyw7 values during summer and autumn with a significant
450 difference ($p < 0.05$) to spring and winter. The mountainous agriculturally dominated catchment
451 (catchment 4), which has the shortest simulation and measurement time series (2020-2021, 2
452 years), shows a somewhat different pattern with only small differences between the three
453 categories during spring and autumn. In summer and winter, on the contrary, Fyw7 shows the
454 same pattern as in all the other catchments. Considering the time series, Fyw7 is lowest for most
455 of the catchments during spring, while Fyw7 is highest during winter. During summer and
456 autumn, the distribution of Fyw7 is similar across all catchments (Fig. 7: green boxplots).
457

458



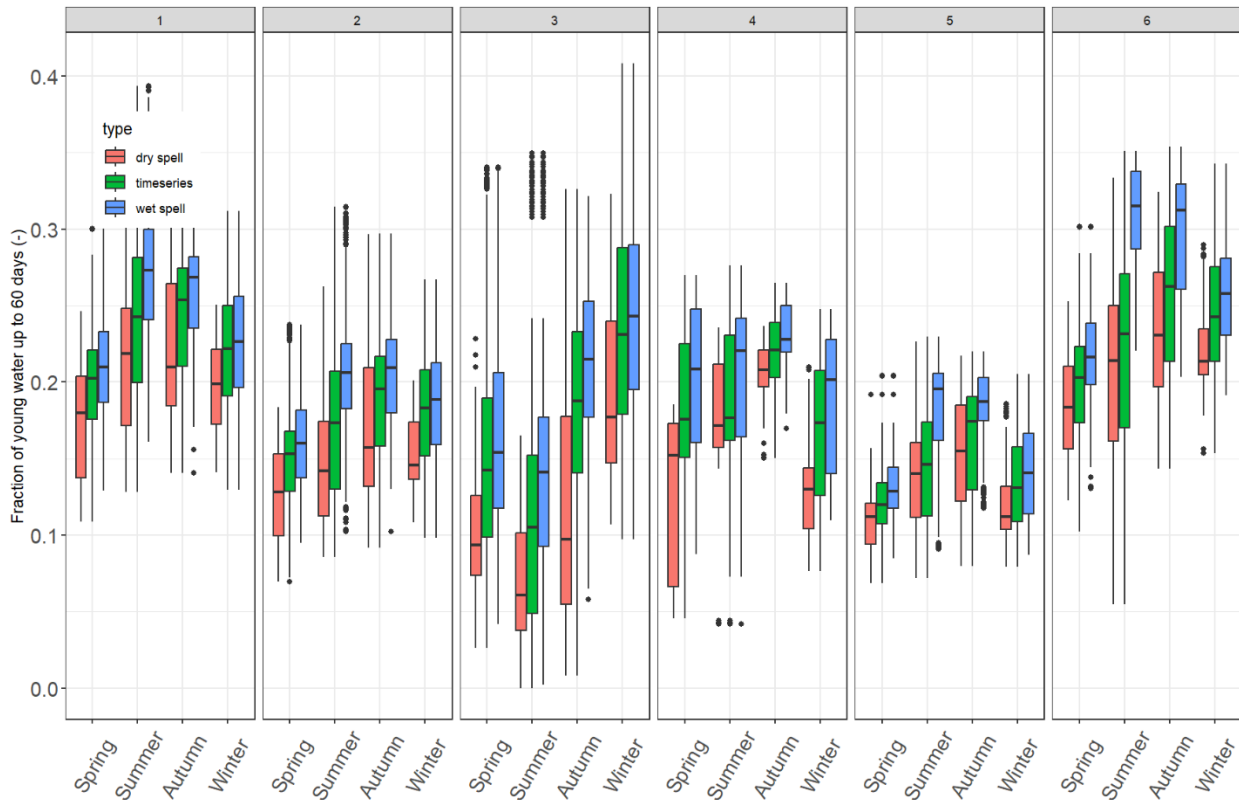
459

460 *Figure 7: Focusing on the Fyw7 (Fractions of young water up to 7 days), boxplots are plotted*
 461 *for dry spells (red), time series (green) and wet spells (blue) during the seasons (Spring,*
 462 *Summer, Autumn and Winter)*

463 For four out of six catchments a significant difference ($p < 0.05$) between the seasons is obvious
 464 with respect to Fyw60 (Fig. 8). The anthropogenic catchment (catchment 2) and the agricultural
 465 lowland headwater catchment (catchment 6) do not show a significant difference of Fyw60
 466 between the seasons summer and autumn for wet spells, while the mountainous agriculturally
 467 dominated catchment (catchment 4) does not show a significant difference of Fyw60 between
 468 spring and winter for both wet and dry spells. This implies that catchment 4 has similar sources
 469 of water during winter and spring. Likewise, for wet spells in summer, the Fyw60 does not differ
 470 significantly from wet spells during spring in the same catchment supporting the assumption that
 471 similar water sources are active during these periods. Considering catchment 4 has the shortest
 472 observation period, which started in 2020 after the drought years 2018 and 2019, it is most likely
 473 that the seasonal differences in Fyw60 that can be seen in the other catchments become apparent

474 because of the longer observation periods that reveal a broader range of different climatic
 475 conditions and a more systematic perspective compared to catchment 4. In the anthropogenic
 476 catchment (catchment 2), the difference between Fyw60 of dry spells during spring and autumn
 477 is not significant.

478



479

480 *Figure 8: Focusing on the Fyw60 (Fractions of young water up to 60 days), boxplots are plotted*
 481 *for dry spells (red), time series (green) and wet spells (blue) during the seasons (Spring,*
 482 *Summer, Autumn and Winter)*

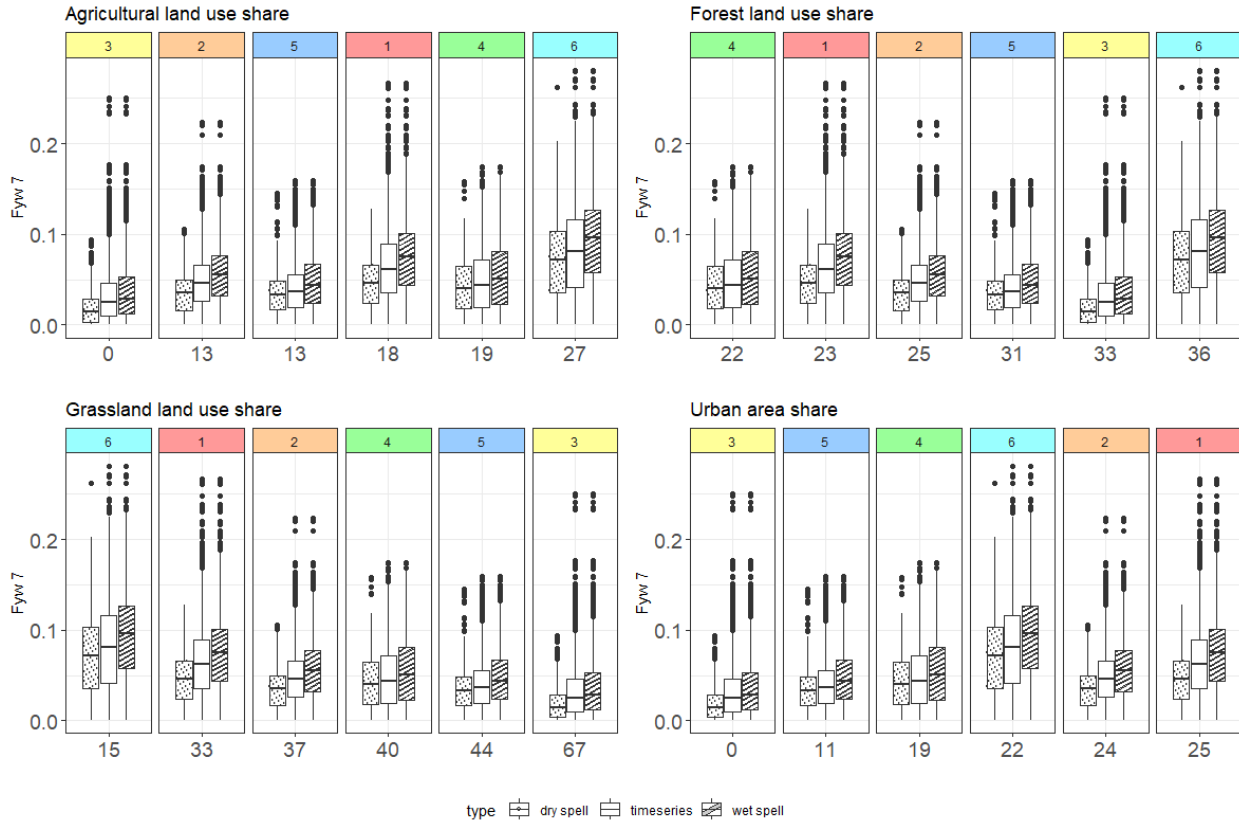
483 In agreement with a conceptual perspective, the findings of our study match the common
 484 expectations that higher contributions of young water (Fyw7 and Fyw60) were found for wet
 485 spells than for dry spells. While this behavior was occurring throughout the time series from
 486 2013 to 2021 for all the six catchments that have been investigated, a much higher contribution
 487 of Fyw7 during summer wet spells was found for two of the six catchments. In the agricultural
 488 lowland headwater catchment (catchment 6) as well as in the forested, hilly catchment
 489 (catchment 5), Fyw7 was higher compared to the other seasons, which indicates that wet spells

490 with high discharge during summer are mainly fed by recent precipitation events. These
491 observations are in line with findings from other studies (Brown, McDonnell et al. 1999, Lee,
492 Shih et al. 2020). Brown et al. (1999) investigated five summer rain events in seven different
493 catchments with the aim to evaluate the storm runoff components and the effect of catchment
494 size on water sources. Using a two-component hydrograph separation to analyze the contribution
495 of water sources during rain events, they were able to show that there were high event water
496 contributions to stormflow for the most intense event and that during dry spells event water is a
497 major contributor to stormflow. Lee et al. (2020) analyzed six typhoons during a 3-year period
498 and found out that higher rainfall intensity causes a higher amount of event water which lowers
499 the mean transit time (MTT).

500 3.4 Catchment characteristics influence extent of discharge age distribution

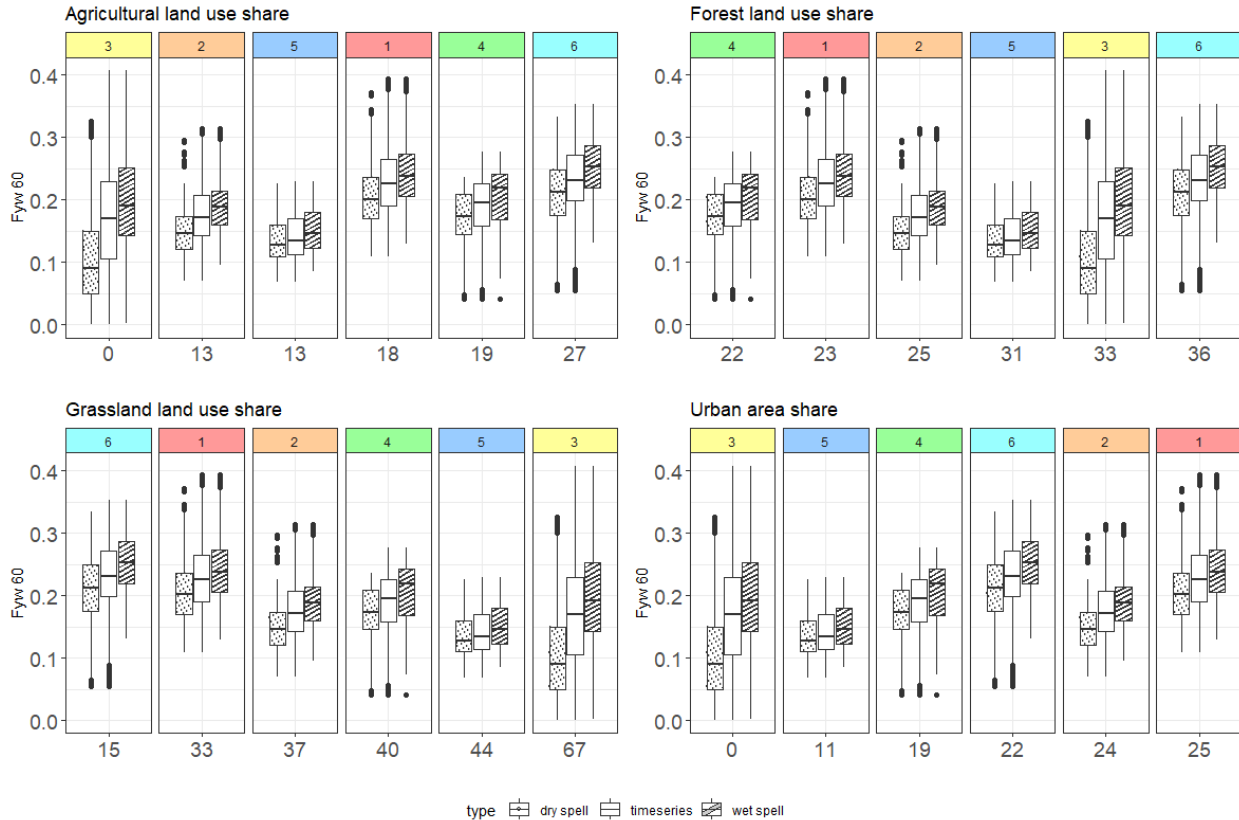
501 A comparison of the relationship between different land use types (agriculture, forest, grassland
502 and urban) and Fyw7 revealed trends for agriculture and grassland depending on their relative
503 proportions (Figure 9). With increasing agricultural land use share the Fyw7 increases
504 significantly ($p < 0.05$, $R^2 = 0.82$; Fig. 9) while the Fyw7 increases when the proportion of
505 grassland decreases in catchments ($p > 0.05$, $R^2 = 0.90$; Fig. 9). Considering the urban land use
506 share, the pattern and trend is similar to the one of agricultural land use share: here again the
507 Fyw7 increases with increasing urban land use share ($p > 0.05$, $R^2 = 0.56$; Fig. 9). For catchment
508 characteristics such as catchment area, slope, gradient, baseflow index, mean elevation and flow
509 path length, significant yet unsystematic differences of the Fyw7 for the different catchments
510 were found (Supp. Fig. 1). For the anthropogenic catchment (catchment 2) and the mountainous
511 agriculturally dominated catchment (catchment 4) the differences of Fyw7 according to their
512 mean elevation, catchment area, gradient, flow path length and baseflow index were not
513 significant.

514



515
 516 *Figure 9: Fyw7 for different catchment characteristics (land use share [%]): agriculture, forest,*
 517 *grassland and urban area) with boxplots representing dry spells (dots), the entire time series*
 518 *(blank) and wet spells (stripes).*

519 For Fyw60, the pattern of increasing fraction of young water with increasing agricultural land
 520 use share as well as the increasing fraction of young water with decreasing grassland proportion
 521 is not as strong as for Fyw7, but still present (R^2 : agriculture = 0.55; grassland = 0.41) (Fig. 10).
 522 This suggests that the release of water from previous rainfall events, such as Fyw7 is more
 523 dependent on land use and land cover characteristics than Fyw60. Hence, one can assume that
 524 agriculturally dominated catchments are in general more sensitive to short term precipitation
 525 events as agriculturally dominated catchments release predominantly young water from recent
 526 precipitation rather than from deeper water sources, which is supported by results from Jasechko
 527 et al. (2016), who found out that agriculturally dominated catchments release more young water
 528 than catchments with other landscape characteristics.



529

530 *Figure 10: Fyw60 for different catchment characteristics (land use share [%]: agriculture,*
 531 *forest, grassland and urban area) with boxplots representing dry spells (dots), the entire time*
 532 *series (blank) and wet spells (stripes).*

533 Our data suggests that there is no direct relation between Fyw7 and the catchment area. This is in
 534 line with other studies that did not find a relation between transit time metrics and catchment
 535 area (Brown, McDonnell et al. 1999, Tetzlaff, Seibert et al. 2009, Lutz, Krieg et al. 2018, Lee,
 536 Shih et al. 2020). While Jutebring Sterte, Lidman et al. (2021) were able to show a relationship
 537 between the catchment size and MTT as well as Fyw up to 2-3 months, they highlighted that the
 538 catchment size is only correlating with the age metrics due to soil types with low conductive silty
 539 sediments and the areal coverage of mires. To analyze the sensitivity of young water up to 2-3
 540 months to hydro-climatic forcing and landscape properties, von Freyberg, Allen et al. (2018a)
 541 investigated 22 Swiss catchments with catchment areas ranging from 0.7 to 351 km². They
 542 revealed that the catchment area correlated with Fyw only with the lower elevation catchments
 543 and the catchments that are not dominated by snow. However, they found a relationship between
 544 Fyw and the areal fraction of saturated soils and low permeability soils which is in line with the

545 findings from Dimitrova-Petrova et al. (2020) and Jutebring Sterte, Lidman et al. (2021).
546 Considering the six catchments of our study, they have a broad variety of different soil types
547 such as luvisols, brown earth, chernozem, gley and sub-types mainly dominated by loess and
548 clay as well as silt; all of these soil types have a low permeability. Lutz, Krieg et al. (2018)
549 already investigated the relationship between water age metrics and catchment characteristics
550 such as soil types, flow path length, catchment area and other catchment characteristics in the
551 Bode region, where our study is conducted as well. They found out that there is no relationship
552 between the catchment characteristics and the Fyw up to 2-3 months during the observed time
553 series from 2013 to 2015. In our study, a weak relationship between Fyw60 and land use types
554 such as grassland and agriculture has been found for the six selected catchments, but for other
555 catchment characteristics such as slope, gradient, mean elevation, flow path length and
556 catchment area we did not find a relation either. Our analysis revealed a positive trend of
557 increasing fractions of young water up to 7 days for an increasing share of agricultural fields
558 with respect to a maximum of agricultural land use about 27 %, whereas a negative trend was
559 found for Fyw7 with an increasing share of grassland, considering that maximum grassland share
560 is 67 % in the investigated catchments. These relationships are stronger for Fyw7 than for Fyw60
561 in our catchments.

562 A positive relation between agricultural land use share and increasing Fyw has also been found
563 by Jasechko et al. (2016), who investigated 254 catchments globally in terms of the contribution
564 of Fyw in stream networks. Agricultural land is mainly different from grassland with respect to
565 soil cultivation and the plant cultures growing on the fields. To maintain a plant-favorable soil
566 environment by directing water from rain events immediately from fields to streams, drainage
567 pipes are built in many cases. By this, the travel time of water through the system is shortened. In
568 other studies, a relation between the drainage density and water age metrics such as MTT and
569 Fyw up to 2-3 months was found (Soulsby, Tetzlaff et al. 2010, von Freyberg, Allen et al. 2018,
570 Dimitrova-Petrova et al., 2020). It is thus possible that the drainage network causes the positive
571 relationship between agricultural land use share and the fraction of Fyw7. Since water table
572 management is not mandatory for cultivated grassland used as meadows as well as for grassland
573 that is part of environmental protection areas, the density of artificial drains in such grassland
574 areas is often low or non-existent. By this, grassland areas can hold back more water (from
575 recent precipitation events) before it is released to the stream network (Zhang & Yang, 2022).

576 Therefore, the decreasing trend of Fyw7 with increasing grassland share in catchments is most
577 likely caused by the buffer capacity of the meadows, mires and environmental protection areas.
578 Since underlying geology has an influence on the landscape structure as well as elevation, it
579 cannot be ruled out that there might be a co-relationship that governs the visible relationship
580 between the land use and Fyw7. Combing the information from all investigated catchments, we
581 did not find any correlation between the contribution of Fyw7 and catchment characteristics such
582 as the slope, elevation or gradient. Despite the missing correlation, we found significant
583 differences of Fyw7 for all catchments that are in turn quite divers with respect to their natural
584 catchment properties like slopes, gradients and mean elevations. To gain more insights into the
585 systematics of the relationship between Fyw7 and catchment characteristics, more detailed
586 information about catchments such as drainage intensity as well as an extended catchment
587 intercomparison study with more investigation areas in different locations from different climatic
588 regions seem necessary.

589 **4 Conclusions**

590 An elaborate high-frequency water isotope monitoring program of stream flow and precipitation
591 was conducted in six different catchments in the Harz mountains and the adjacent northern
592 lowlands, Germany, in order to investigate the relation between age metrics (fractions of
593 different water ages, transit times) and catchment characteristics (discharge, landscape structure
594 metrics). Special focus was put on hydrological divergent periods. Water age metrics are
595 obtained by the tran-SAS model (Benettin and Bertuzzo, 2018) with daily input data. Discharge
596 sensitivities of water parcels with an age of up to 7 and 60 days were obtained using the
597 approach after Gallart et al. (2020), revealing the highest sensitivity for an agriculturally
598 dominated headwater catchment. Generally, agriculturally dominated catchments are likely to
599 release more young water (Jasechko et al., 2016). Consequently, in the context of pollution
600 awareness and pollution control, special attention should be paid to those catchments that are
601 characterized by high shares of agricultural area. This is due to the fact that pollutants (e.g.
602 pesticides) and other solutes (nutrients) can quickly reach the streams with higher fractions of
603 young water. Resulting short transit times may not sustain natural retention or degradation of
604 contaminants posing a potential risk to the streams as the primary receptors of young water
605 shares. With increasing share of grassland, Fyw7 decreases, which indicates that landscape

606 structures affect the hydrological conditions of streams. Probably, higher amounts of grassland as
607 well as more grassland patches between agricultural fields could have a reverse effect on the
608 release of young water by holding back younger water proportions and supporting the infiltration
609 to deeper storages. This might create a positive side effect with respect to pollution control by
610 facilitating longer travel times and, as a consequence, an enhanced pollutant degradation
611 potential. However, especially in Central and Western Europe, climate change impacts will result
612 in more frequent rainfall events after prolonged dry conditions leading to a scenario with more
613 dominant release of young water increasing the pollution risk of the streams. The assumption of
614 such a scenario is supported by the findings of this study with respect to increasing amounts of
615 young water, both F_{yw60} and F_{yw7} , from summer to autumn. This behavior might result from
616 the catchment storage drying out during prolonged dry spells resulting in less mixing between
617 water sources in the subsurface. Catchments with high discharge peaks were prone to have lower
618 discharge sensitivities for F_{yw7} compared to F_{yw60} , indicating that these catchments are more
619 affected by increasing discharge and react more quickly to increasing discharge with higher
620 fractions of young water from preceding precipitation. As expected, the analysis of high and low
621 flows revealed higher contributions of young water during wet spells compared to dry spells
622 considering daily data of each wet/ dry spell.

623 Considering their large potential variability on a regional or even global scale, the hydro-climatic
624 properties of the six investigated catchments were in a quite narrow range. To some extent, this
625 hampers the recognition of the systematic relationships between catchment characteristics and
626 fractions of young water. We believe that significant additional knowledge gain can be expected
627 if the selected catchments reflect a much broader range of catchment characteristics and hydro-
628 climatic properties knowing though that such an approach would be associated with enormous
629 logistical challenges. However, one of the valuable contributions of our study is that it could
630 serve as a blueprint for further investigations aiming at the recognition of hydrological processes
631 and the age distribution of stream water during divergent hydrological periods in a more global
632 context. Upcoming studies should in particular pay attention to the differing tendency of
633 catchments to release water from previous precipitation events and water that is categorized as
634 young water with an age around 2-3 months as this young water share carries the main pollution
635 risk.

636 Understanding how catchments react during differing hydrological conditions and the
637 implementation of this understanding into land management actions is crucial for controlling
638 nutrient losses and pollution risks of streams especially in the view of the projected climate
639 change. As shown by this study, high-frequency isotope monitoring programs in concert with the
640 application of appropriate transit time models can significantly contribute to enlarge this
641 understanding.

642 **Acknowledgments**

643 There is no conflict of interest for any author.

644 Monitoring set up was implemented by KK and CM. Samples were collected by KK and CM,
645 while sample preparation and laboratory isotope analysis were conducted by CR and laboratory
646 staff of the Helmholtz-Centre for Environmental Research in Halle, Germany. The study was
647 developed by CR, KK, SL and RM. The mHM-model was set up and run by RK, while the tran-
648 SAS models for each catchment were set up and run by CR. Data analysis (statistics, discharge
649 sensitivity) was conducted by CR. The manuscript was written by CR, while all other co-authors
650 reviewed the manuscript.

651
652 We are grateful for the support by Jana von Freyberg, who gave helpful advice on the
653 implementation of the discharge sensitivity approach for fractions of young water derived from
654 tran-SAS. We would like to thank Paolo Benettin for being the contact person in terms of
655 questions with regard to the tran-SAS v1.0 model.

656
657 **Open Research**

658 Datasets including isotope measurements and the mHM-simulations of all six catchments are
659 stored for the purposes of peer review process at the UFZ-nextcloud accessible via the following
660 link and password: <https://nc.ufz.de/s/yz6pMACGFikaxKx> ,password: *WRR_23_Radtke*. By the
661 time the article is accepted the data will be made publicly available with a DOI via the
662 datainvestigationportal of the Helmholtz-Centre for Environmental Research
663 (<https://www.ufz.de/drp/en/>). Water age metrics can be derived using the tran-SAS model
664 (Benettin & Bertuzzo, 2018: <https://doi.org/10.5194/gmd-11-1627-2018> (article) and
665 <https://github.com/pbenettin/tran-SAS> (source code)) with the data provided and the parameters
666 mentioned in the paper.

667
668 **References**

669 BGR. (2020). Bodenübersichtskarte. Bundesanstalt für Geowissenschaften und Rohstoffe.
670 BGR. (2020). Hydrogeologische Übersichtskarte. Bundesanstalt für Geowissenschaften und
671 Rohstoffe.

- 672 Benettin, P. and E. Bertuzzo (2018). "tran-SAS v1.0: a numerical model to compute catchment-
673 scale hydrologic transport using StorAge Selection functions." *Geoscientific Model*
674 *Development* 11(4): 1627-1639.
- 675
- 676 Borriero, A., Kumar, R., Nguyen, T. V., Fleckenstein, J. H., and Lutz, S. R.: Uncertainty in water
677 transit time estimation with StorAge Selection functions and tracer data interpolation,
678 *Hydrol. Earth Syst. Sci. Discuss.* [preprint], <https://doi.org/10.5194/hess-2022-222>, in
679 review, 2022.
- 680
- 681 Brown, V. A., J. J. McDonnell, D. A. Burns and C. Kendall (1999). "The role of event water, a
682 rapid shallow flow component, and catchment size in summer stormflow." *Journal of*
683 *Hydrology*.
- 684 Dimitrova-Petrova, K., J. Geris, M. E. Wilkinson, A. Lilly and C. Soulsby (2020). "Using
685 isotopes to understand the evolution of water ages in disturbed mixed land-use
686 catchments." *Hydrological Processes* 34(4): 972-990.
- 687 DWD Climate Data Center (CDC): Historische tägliche Stationsbeobachtungen (Temperatur,
688 Druck, Niederschlag, Sonnenscheindauer, etc.) für Deutschland, Version v21.3, 2021.
- 689 GeoBasis-DE / BKG. (2013). Elevation data 200m resolution. Bundesamt für Kartographie und
690 Geodäsie.
- 691 GeoBasis-DE / BKG. (2018). Land-use data. Bundesamt für Kartographie und Geodäsie.
- 692 Gupta, H. V., H. Kling, K. K. Yilmaz and G. F. Martinez (2009). "Decomposition of the mean
693 squared error and NSE performance criteria: Implications for improving hydrological
694 modelling." *Journal of Hydrology* 377(1-2): 80-91.
- 695 Hrachowitz, M., C. Soulsby, D. Tetzlaff, J. J. C. Dawson and I. A. Malcolm (2009).
696 "Regionalization of transit time estimates in montane catchments by integrating
697 landscape controls." *Water Resources Research* 45(5).
- 698 Jasechko, S., J. W. Kirchner, J. M. Welker and J. J. McDonnell (2016). "Substantial proportion
699 of global streamflow less than three months old." *Nature Geoscience* 9(2): 126-129.

- 700 Jutebring Sterte, E., F. Lidman, E. Lindborg, Y. Sjöberg and H. Laudon (2021). "How catchment
701 characteristics influence hydrological pathways and travel times in a boreal landscape."
702 *Hydrology and Earth System Sciences* 25(4): 2133-2158.
- 703 Kaur, S., A. Horne, M. J. Stewardson, R. Nathan, A. M. Costa, J. M. Szemis and J. A. Webb
704 (2017). "Challenges for determining frequency of high flow spells for varying thresholds
705 in environmental flows programmes." *Journal of Ecohydraulics* 2(1): 28-37.
- 706 Kirchner, J. W. (2016a). "Aggregation in environmental systems – Part 1: Seasonal tracer cycles
707 quantify young water fractions, but not mean transit times, in spatially heterogeneous
708 catchments." *Hydrology and Earth System Sciences* 20(1): 279-297.
- 709 Kirchner, J. W. (2016b). "Aggregation in environmental systems – Part 2: Catchment mean
710 transit times and young water fractions under hydrologic nonstationarity." *Hydrology and
711 Earth System Sciences* 20(1): 299-328.
- 712 Kirchner, J. (2018). "Quantifying new water fractions and transit time distributions using
713 ensemble hydrograph separation: theory and benchmark tests." *Hydrol Earth Syst Sci.*
- 714 Knapp, J. L. A., Neal, C., Schlumpf, A., Neal, M., and Kirchner, J. W. (2019): New water
715 fractions and transit time distributions at Plynlimon, Wales, estimated from stable water
716 isotopes in precipitation and streamflow, *Hydrol. Earth Syst. Sci.*, 23, 4367–4388,
717 <https://doi.org/10.5194/hess-23-4367-2019>.
- 718 Kumar, R., L. Samaniego and S. Attinger (2013). "Implications of distributed hydrologic model
719 parameterization on water fluxes at multiple scales and locations." *Water Resources
720 Research*.
- 721 Kundzewicz, Z. W., S. Kanae, S. I. Seneviratne, J. Handmer, N. Nicholls, P. Peduzzi, R.
722 Mechler, L. M. Bouwer, N. Arnell, K. Mach, R. Muir-Wood, G. R. Brakenridge, W.
723 Kron, G. Benito, Y. Honda, K. Takahashi and B. Sherstyukov (2013). "Flood risk and
724 climate change: global and regional perspectives." *Hydrological Sciences Journal* 59(1):
725 1-28.

- 726 Kuppel, S., D. Tetzlaff, M. P. Maneta and C. Soulsby (2018). "EcH²O-iso 1.0: water isotopes
727 and age tracking in a process-based, distributed ecohydrological model." *Geoscientific*
728 *Model Development* 11(7): 3045-3069.
- 729 Ladson, A. R., R. Brown, B. Neal and R. Nathan (2013). "A standard approach to baseflow
730 separation using the Lyne and Hollick filter." *Australian Journal of Water Resources*
731 17(1).
- 732 Landesbetrieb für Hochwasserschutz und Wasserwirtschaft. (10. 10 2022).
733 *Hochwasservorhersagezentrale*. Von [https://hochwasservorhersage.sachsen-](https://hochwasservorhersage.sachsen-anhalt.de/messwerte/durchfluss/?no_cache=1)
734 [anhalt.de/messwerte/durchfluss/?no_cache=1](https://hochwasservorhersage.sachsen-anhalt.de/messwerte/durchfluss/?no_cache=1) abgerufen
- 735 Lang, M., T. B. M. J. Ouarda, and B. Bobée (1999), Towards operational guidelines for over-
736 threshold modeling, *J. Hydrol.*, 225, 103– 117.
- 737
- 738 Lee, J.-Y., Y.-T. Shih, C.-Y. Lan, T.-Y. Lee, T.-R. Peng, C.-T. Lee and J.-C. Huang (2020).
739 "Rainstorm Magnitude Likely Regulates Event Water Fraction and Its Transit Time in
740 Mesoscale Mountainous Catchments: Implication for Modelling Parameterization."
741 *Water* 12(4).
- 742 Lutz, S. R., R. Krieg, C. Müller, M. Zink, K. Knöller, L. Samaniego and R. Merz (2018).
743 "Spatial Patterns of Water Age: Using Young Water Fractions to Improve the
744 Characterization of Transit Times in Contrasting Catchments." *Water Resources*
745 *Research* 54(7): 4767-4784.
- 746 Lyne, V. and M. Hollick (1979). "Stochastic Time-Variable Rainfall Runoff Modelling."
747 Institute of Engineers Australia National Conference.
- 748 Lyon, S. W., S. W. Ploum, Y. van der Velde, G. Rocher-Ros, C.-M. Mörth and R. Giesler
749 (2018). "Lessons learned from monitoring the stable water isotopic variability in
750 precipitation and streamflow across a snow-dominated subarctic catchment." *Arctic,*
751 *Antarctic, and Alpine Research* 50(1).

- 752 Merz, R., Blöschl, G., & Parajka, J. (2006). Spatio-temporal variability of event runoff
753 coefficients. *Journal of Hydrology*, 331(3–4), 591–604.
754 <http://doi.org/10.1016/j.jhydrol.2006.06.008>
- 755 Michelsen, N., G. Laube, J. Friesen, S. Weise, A. Said and T. Müller (2019). „Technical note: A
756 microcontroller-based automatic rain sampler for stable isotope studies”. *Hydrology and*
757 *Earth System Sciences*. 23. 2637-2645.
- 758 Mueller, C., Zink, M., Samaniego, L., Krieg, R., Merz, R., Rode, M. and Knöller, K., 2016.
759 Discharge driven nitrogen dynamics in a mesoscale river basin as constrained by stable
760 isotope patterns. *Environmental Science & Technology*, 50(17), pp.9187-9196.
- 761 Samaniego, L., R. Kumar and S. Attinger (2010). "Multiscale parameter regionalization of a
762 grid-based hydrologic model at the mesoscale." *Water Resources Research*.
- 763 Sikorska, A. E., Viviroli, D., & Seibert, J. (2015). Flood-type classification in mountainous
764 catchments using crisp and fuzzy decision trees. *Water Resources Research*, 51(10),
765 7959–7976. <http://doi.org/10.1002/2015WR017326>
- 766 Soulsby, C., D. Tetzlaff and M. Hrachowitz (2010). "Are transit times useful process-based tools
767 for flow prediction and classification in ungauged basins in montane regions?"
768 *Hydrological Processes*.
- 769 Soulsby, C., D. Tetzlaff, P. Rodgers, S. Dunn and S. Waldron (2006). "Runoff processes, stream
770 water residence times and controlling landscape characteristics in a mesoscale catchment:
771 An initial evaluation." *Journal of Hydrology* 325(1-4): 197-221.
- 772 Stockinger, M. P., H. R. Boga, A. Lücke, B. Diekkrüger, T. Cornelissen and H. Vereecken
773 (2016). "Tracer sampling frequency influences estimates of young water fraction and
774 streamwater transit time distribution." *Journal of Hydrology* 541: 952-964.
- 775 Tang, W. and S. K. Carey (2017). "HydRun: A MATLAB toolbox for rainfall-runoff analysis."
776 *Hydrological Processes* 31(15): 2670-2682.

- 777 Tetzlaff, D., J. Seibert, K. J. McGuire, H. Laudon, D. A. Burns, S. M. Dunn and C. Soulsby
778 (2009). "How does landscape structure influence catchment transit time across different
779 geomorphic provinces?" *Hydrological Processes* 23(6): 945-953.
- 780 von Freyberg, J., B. Studer and J. W. Kirchner (2017). "A lab in the field: high-frequency
781 analysis of water quality and stable isotopes in stream water and precipitation."
782 *Hydrology and Earth System Sciences* 21(3): 1721-1739.
- 783 von Freyberg, J., S. T. Allen, S. Seeger, M. Weiler and J. W. Kirchner (2018a). "Sensitivity of
784 young water fractions to hydro-climatic forcing and landscape properties across 22 Swiss
785 catchments." *Hydrology and Earth System Sciences* 22(7): 3841-3861.
- 786 von Freyberg, J., B. Studer, M. Rinderer and J. W. Kirchner (2018b). "Studying catchment storm
787 response using event- and pre-event-water volumes as fractions of precipitation rather
788 than discharge." *Hydrology and Earth System Sciences* 22(11): 5847-5865.
789 <https://doi.org/10.5194/hess-22-5847-2018>
- 790 Wilusz, D. C., C. J. Harman and W. P. Ball (2017). "Sensitivity of Catchment Transit Times to
791 Rainfall Variability Under Present and Future Climates." *Water Resources Research*
792 53(12): 10231-10256.
- 793 Wollschläger, U., S. Attinger, D. Borchardt, M. Brauns, M. Cuntz, P. Dietrich, J. H.
794 Fleckenstein, K. Friese, J. Friesen, A. Harpke, A. Hildebrandt, G. Jäckel, N. Kamjunke,
795 K. Knöller, S. Kögler, O. Kolditz, R. Krieg, R. Kumar, A. Lausch, M. Liess, A. Marx, R.
796 Merz, C. Mueller, A. Musolff, H. Norf, S. E. Oswald, C. Rebmann, F. Reinstorf, M.
797 Rode, K. Rink, K. Rinke, L. Samaniego, M. Vieweg, H.-J. Vogel, M. Weitere, U.
798 Werban, M. Zink and S. Zacharias (2016). "The Bode hydrological observatory: a
799 platform for integrated, interdisciplinary hydro-ecological research within the TERENO
800 Harz/Central German Lowland Observatory." *Environmental Earth Sciences* 76(1).
- 801 Zhang, L.; Yang, F. "Spatio-Temporal Dynamics of Water Conservation Service of Ecosystems
802 in the Zhejiang Greater Bay Area and Its Impact Factors Analysis." *Sustainability* 2022,
803 14, 10392. <https://doi.org/10.3390/su141610392>

804 Zink, M., Kumar, R., Cuntz, M., and Samaniego, L.: A high-resolution dataset of water fluxes
805 and states for Germany accounting for parametric uncertainty, *Hydrol. Earth Syst. Sci.*,
806 21, 1769–1790, <https://doi.org/10.5194/hess-21-1769-2017>, 2017.

807